Distance over Time in a Maximal Sprint: Understanding Athletes' Action Boundaries in Sprinting

Dees B.W. Postma[a,c]*; Martijn B. Wieling[b]; Koen A. P. M. Lemmink[c] and Frank T.J.M. Zaal[c]

[a]Human Media Interaction, University of Twente, Enschede, The Netherlands; [b]Humanities Computing, University of Groningen, Groningen, The Netherlands; [c]Department of Human Movement Sciences, University Medical Center Groningen, University of Groningen, The Netherlands

*d.b.w.postma@utwente.nl

Distance over Time in a Maximal Sprint: Understanding Athletes' Action Boundaries in Sprinting

The present study examined the kinematics of maximal effort sprint running, mapping the relations among a person's maximal running speed, maximum running acceleration and the distance coverable in a certain amount of time by this person. Thirty-three participants were recruited to perform a simple sprint task. Both forward and backward running were considered. Participants' position, velocity and acceleration data were obtained using a Local Positioning Measurement system. Participants' speed-acceleration profiles turned out to be markedly *non-linear*. To account for these non-linear patterns, we propose a new macroscopic model on the kinematics of sprint running. Second, we examined whether target distance was of influence on the evolution of participants' running speeds over time. Overall, no such effect on running velocity was present, except for a 'finish-line effect'. Finally, we studied how variation in individuals' maximum running velocities and accelerations related to differences in their action boundaries. The findings are discussed in the context of affordance-based control in running to catch fly balls.

Keywords: action boundaries; sprinting; interception; Generalized Additive Modelling

Introduction

Will he be able to make that catch? Spectators of baseball games, for instance, might watch a running outfielder with excitement, eager to find out the answer to this question. Will he be able to reach the ball before it hits the ground? Given his abilities, will the outfielder have enough time to reach the location where the ball will land? Expressed in this way, it is clear that the affordance of interceptability should be captured by the relations among the outfielder's running abilities, the distance to be covered and the time before the ball hits the ground (Oudejans et al., 1996; Postma et al., 2018; Steinmetz et al., 2020). The present contribution addresses these relations. More specifically, we ask the question of how much time is needed to cover a certain distance (or, alternatively, how much distance can be covered in a certain time), and how this is related to the maximum running speed and running acceleration that a person can attain. The issue is broader than situations of interception of projectiles such as balls: think of examples such as crossing streets (Oudejans et al., 1996) and catching busses. What all these situations have in common is that they all revolve around the issue of being at some place in the right time or trying to avoid this.

The issue of what determines the maximum distance that can be covered in a fixed time has been addressed primarily in studies into fly-ball catching. The results from these studies (Fajen et al., 2011; Oudejans et al., 1996; Postma et al., 2018) seem to suggest that it is not a person's maximum speed nor his or her maximum acceleration per se that determines the action boundary of running. For example, Oudejans and colleagues (1996) determined the boundary between catchable and uncatchable fly balls (or fly balls judged as such). In their analyses, distance-over-time (i.e. required velocity) and distance-over-time-squared (i.e. required acceleration) better captured the observed boundaries than distance did, whereas the fits based on these velocity and acceleration measures were of similar quality. Fajen et al. (2011), in a follow-up on the Oudejans et al. (1996) study, introduced an alternative to the required-velocity measure. They determined, per participant, at each point in time the greatest distance that the participant had covered. They used this to compute, for each trial, the difference in the time needed to cover the distance to the ball's landing location and flight time of the ball, which was called 'time-to-spare'. Using this time-to-spare as a basis for drawing the boundaries between catchable and uncatchable balls led to similar results as using required velocity (for the conditions that were compared, see Fajen et al., 2011). Finally, Postma and colleagues (2018) used the maximum distance that a participant had been able to cover during the flight time of the balls (which was roughly constant in their experiment) to characterize the boundary between catchable and uncatchable fly balls. Their analyses showed that this 'locomotor range' led to better fits than required velocity or required acceleration. Taken together, these studies indicate that the distance that players can run in a certain time does not seem to be determined exclusively by either the maximum velocity or the maximum acceleration that they are able to reach. Still, both variables seem to play a role in defining this maximum distance.

Already in 1927, Hill and colleagues studied the dynamics of sprint running, specifically in the context of athletics (Furusawa et al., 1927; Hill, 1927). Hill and colleagues derived a mono-exponential relationship that described the velocity-time relation of an athletes' center of mass in maximal-effort sprinting. From their model it is predicted 1) that maximal acceleration is seen right at the start of the run and 2) that an inverse linear relationship exists between running speed and acceleration. While proven effective for athletics, Hill's characterization of sprint running seems not readily applicable to the context of locomotor interception tasks. First, because agents in locomotor interception tasks are typically unaided by starting blocks and secondly because the direction of motion is not always known *a priori*

(e.g., in baseball, an outfielder does not know which way to run until the ball is hit). We expect that this will mean that players will not reach their maximum acceleration instantaneously but probably somewhat later in the run. The implication of this would be that the relation between acceleration and velocity, when asking players to run at their maximum abilities, will not be entirely linear either (we expressly investigate this below). Furthermore, some interception tasks might require agents to run in other directions than the forward-direction. Running *backwards* to intercept a ball or an opponent is common in sports like soccer, basketball, and football but is not explicitly covered by the Hill model. Finally, the task ecology of the aforementioned sports settings is different from athletic sprinting. Indeed, in many team sports, sprints are typically short and explosive; seldomly do athletes sprint for hundred meters or more. This difference in task (ecology) might impact the way they cover a certain distance to make an interception. Thus, to characterize the action boundaries in interceptive tasks, further investigation into the macro-dynamics of running is required – for short and long distances, running backwards and forwards.

To map the relation among maximum velocity, maximum acceleration, and the distance coverable within a certain timeframe, we designed a simple sprinting experiment that was general enough to shed light on agents' action boundaries for various interceptive tasks, yet specific enough to represent those tasks. We collected data of participants performing maximal-effort sprints. No starting blocks were used, and we examined different modes of locomotion (forwards and backwards) and different target distances. As a first objective, we set out to examine whether an inverse linear relationship was indeed apparent for sprinting in the forward direction. The results show that maximal running speed is *non-linearly* related to acceleration in the context of the current sprinting task. This was the case for all target distances (7.5 meters – 60 meters). To account for these non-linear patterns, we propose a new macroscopic model on the kinematics of sprint running. This new model also explicitly covers the macro-dynamics of *backward sprinting*, a mode of locomotion common in many (sports related) interceptive tasks. Model performance is evaluated for both forward sprinting and backward sprinting. We show that our alternative model provides an accurate characterization of the dynamics of running. As such, it shows to be promising for understanding agents' action boundaries in various interceptive tasks.

Methods

Participants

Thirty-three people (30 men and 3 women) participated in this study. On average, participants were 21 years old (SD = 1.2). Participants were healthy individuals and reported no injuries that could affect their performance during the experiment. All participants had prior experience with running on artificial grass, for example in the context of (recreational) soccer or field hockey. Prior to the experiment, all participants were informed about the procedure of the experiment both in writing and orally. The experiment was approved by the Ethics Committee of the Center for Human Movement Sciences (University Medical Center Groningen, the Netherlands), and the protocol was in accordance with the Declaration of Helsinki.

Setup and apparatus

The experiment took place on artificial turf at one of the practice fields of a professional soccer club (FC Groningen, The Netherlands). Participants carried out their sprints in (randomized) groups of three to six people. Participants were all assigned an individual lane. Every lane was exactly 5 meters wide. Pylons were placed along the long side of the lanes to demarcate different target distances: 3.75, 7.5, 15, 30 and 60 meters. The starting line was the

same over all participants and trials and was set at 0 meters. Right behind the starting line, at the centerline of every lane, a pylon was positioned at minus one meter.

Position data were recorded using the Local Positioning Measurement (LPM-) system (Inmotio Object Tracking B.V., Amsterdam, The Netherlands). Position data were obtained with a sample frequency of 62.5Hz. Two video cameras recorded the experiment: One camera provided close-up footage of the starting line, the other captured the entire field. The camera that made close-up footage of the field was used to record the starting signal for later analysis. Both cameras were Full-HD and recorded the experiment at 30Hz.

Design

The experiment had a repeated-measures, block-randomized design (4 conditions × 4 targets × 2 repetitions). Participants performed a total of 32 maximal-effort sprints over four different conditions. In the *forward-condition* participants were required to cover different distances (7.5, 15, 30 and 60 meters) as fast as possible, sprinting forwards. In the *backward-condition* participants were again required to cover different distances (3.75, 7.5, 15 and 30 meters[1]), however they were now required to do so sprinting backwards. Participants also performed a *'compulsory-turn condition'* and an *'optional-turn condition'*. However, these two conditions will not be considered for the present contribution.

Procedure

The conditions were presented in a fixed sequence: Participants started out with trials from the forward-condition, followed by trials from the backward- and the compulsory-turn conditions to finally perform the last eight trials from the optional-turn condition. Trials from the backward- and the compulsory-turn condition were intermixed and presented in alternating order. For the backward-condition, participants were instructed to keep running until they had the designated finish pylons in their (peripheral) sight, this was to motivate participants to keep up their efforts until they had actually reached the finish line.

For all conditions, participants were required to start from standstill in an upright position with both feet positioned directly underneath their shoulders. When the starting signal was given, they were required to start sprinting immediately. The starting signal was an auditory cue, produced by striking two wooden planks forcefully against each other. This was done out of sight of the participants so no visual anticipation on the start-signal would occur. At the same time, the wooden planks served as a visual cue that could be used in data analysis to demarcate the start of each trial. In between trials, participants were given three minutes rest to allow for sufficient recovery. Also, to avoid injuries, participants were required to perform a scripted and supervised ten-minute, moderate intensity warm-up prior to the experiment.

Data analysis

Raw position-data with timestamps, along with some auxiliary data, like participants' transponder ID's, were imported into MATLAB (MathWorks R2019a) and R (R Core Team, 2019) for further analysis. We intended to use the visual cue, given by one of the experimenters on the field, to demarcate the beginning of each trial, but this turned out not to be viable. With the LPM-software, events of interest could only be marked with limited temporal accuracy (i.e. accurate to about ± 200-300ms). Therefore, the start of every trial was

[1] Note that the series of target distances for backward sprinting is slightly different from the series for forward sprinting. We reasoned that in most interceptive tasks, agents would never run 60 meters backwards. Arguably, agents would neither run 60 meters forwards to make an interception, however we also wanted to sample the extreme cases (e.g. 'The Catch' by Willie Mays – Adair, 2002; p. 101).

taken to be the moment a participant reached a running velocity greater than 1 ms^{-1}. As such, the start of every trial was determined individually, rendering response time to be irrelevant for further analyses. The end of every trial was taken to be the instant participants reached the total distance they had to cover, that is when they reached the finish line.

Linearity between speed and acceleration

As a first objective, we set out to examine whether an inverse linear relation exists between running speed and acceleration, as would be predicted from Hill's (Furusawa et al., 1927; Hill, 1927) mono-exponential relation on athletic sprint running. As the inverse-linear relationship was only explicitly hypothesized for forward running, only trials from the forward-condition were considered for this analysis. Running speed and acceleration were calculated by differentiating participants' position-data. *Generalized Additive Mixed Modelling* (GAMM) was used to test for linearity between running speed and acceleration.

GAMM is a powerful and flexible regression technique (Hastie & Tribshirani, 1990; Wood, 2017). As an extension of mixed-effects regression, it is able to account for nested dependencies in the data. The present experiment is designed such that for every condition, every participant performs two sprints per target distance. As such, part of the variance in the data is inherently linked to individual participants and part of the variance is inherently linked to the different target distances. Mixed-effects regression models (and Generalized Additive Mixed Models, GAMMs, by extension) are able to bring such dependencies into the model, mitigating overconfidence in *p*-values. Furthermore, GAMMs (as implemented in the R package *mgcv*—Wood, 2003, 2004, 2011, 2017; Wood, Pya, & Säfken, 2016) are able to correct for autocorrelation in the residuals, which is crucial in analyzing time-series data. Finally, and perhaps most importantly, GAMMs explicitly allow for nonlinear relationships to be modelled. Frequently, the relation between the dependent variable and independent variables is not linear. Yet, conventional regression techniques typically do not allow for departures from linearity unless the shape of the non-linear pattern is explicitly specified *a priori* (e.g. with quadratic or logarithmic functions). With GAMMs, non-linear patterns in the data can be modelled through 'smooths'. By default, the *mgcv*-package employs thin-plate regression splines to model nonlinear patterns in the data. The degree of smoothness is determined by the number of (increasingly complex non-linear) basis functions that are used to characterize the nonlinear pattern. Rather than fitting the best nonlinear pattern, GAMMs penalize nonlinearity in order to prevent overfitting. The result of this approach is that GAMMs will only identify a nonlinear pattern if there is enough support for its presence in the data (which is also validated internally via cross-validation). One approach to formally test for linearity using GAMMs is to fit and compare two models: One for which the relationship between the dependent and the independent variable is forced to be *linear* and one for which *nonlinear* relationships are also allowed[2]. A model specification *without* smoothing functions will produce a linear model while a model specification *with* smoothing functions will produce a nonlinear model if the data supports it (see also: Wieling, 2018).

For each of the four target distances of the *forward-condition*, both a 'linear' and a 'non-linear model' were created. The latter model allowed for the modelling of non-linear patterns in the data by using a thin-plate regression spline with (at most) ten basis functions. The former model employed no such smoothing functions which forces the relationship between velocity and acceleration to be modelled by a linear function. In this procedure, we only

[2] But note that a generalized additive mixed model which shows a non-linear effect is already evidence for this (as a linear effect would be identified if no nonlinear pattern is present).

considered the best attempt of every participant per target condition. This was done, so that participants' velocity profiles could be normalized in order to prevent spurious fits. Both models were fit using maximum likelihood estimation. This allowed for direct model comparison using the function *compareML* from the *itsadug*-package (van Rij et al., 2017). To account for alpha-inflation due to multiple testing, a Bonferroni correction was applied. Apart from the intended difference in linearity, the model specifications for the linear model and the nonlinear model were the same for all target distances. For more information on the mixed model framework and specifically GAMMs, see for example: Tagliamonte & Baayen, 2012; Wieling, 2018; Winter, 2013; and Winter & Wieling, 2016.

Determining the effect of target distance on participants' velocity profiles

People might cover certain distances differently depending on the total distance that needs to be covered. In our experiment for instance, participants might have covered the first 7.5 meters of a 15-meter dash differently from the first 7.5 meters of a 60-meter dash. As such, we used GAMMs to check for differences in participants' velocity profiles for different target distances. To test for such potential differences, we examined the running data from the forward-condition. With GAMMs, it is possible to identify the range over which two (nonlinear) patterns are significantly different. The velocity profiles over the first 7.5 meters of all target distances were compared; the velocity profiles over the first 15 meters of all but the 7.5-meter target distance were compared and the velocity profiles over the first 30 meters of the 30-meter dash and the 60-meter dash were compared. All trials of all participants were considered.

Results

For final analysis, data from two participants were excluded. Data from one participant was incomplete due to technical difficulties related to one of the LPM-transponders, and one participant had to quit the experiment prematurely due to an unreported, pre-existing injury. As such, the final analysis was performed on data from all trials of the remaining 31 participants.

Linearity of running speed and acceleration

As a first objective, we set out to examine whether Hill's presumed inverse linear relation between running speed and running acceleration in a maximal-effort sprint was present. Figure 1 presents normalized running acceleration as a function of normalized running speed for each of the four target distances[3]. Using GAMMs, both a linear and a nonlinear model were fitted to data from the *forward-condition*. For each of the four target distances (i.e. 7.5, 15, 30 and 60 meters), the nonlinear model provided a significantly better fit to the data than its linear counterpart. The difference between the two models was highly significant with $p < 0.001$ for the 7.5, 15, 30 and 60-meter dash ($\chi^2(1) = 143$; $\chi^2(1) = 155$; $\chi^2(1) = 151$ and $\chi^2(1) = 226$, respectively).

<Figure 1>

The effect of target distance on participants' velocity-profiles

Having established the nonlinearity of the relation between velocity and acceleration, we examined whether target distance influenced participants' sprint behavior. Subtle differences might exist for the way agents cover different distances. Distinct pacing strategies may be

[3] For the creation of Figure 1, velocity and acceleration data have been smoothed using a gaussian filter (see also section '*A new macroscopic model on the kinematics of sprint running*'.

employed for various target distances. To test this, we constructed GAM models to make direct comparisons between different target distances. *Figure 2A* shows velocity profiles of the first 7.5 meters of all trials of the *forward-condition*, for all four target distances. From the fitted velocity profiles (solid lines) with 95% confidence intervals (shaded areas), it can be seen that participants' velocity profiles during their first 7.5 m of running are highly similar for the different target distances. Only a small, but marked, deviation can be observed for the 7.5-meter dash. While the velocity profiles for the 15-meter dash, the 30-meter dash and the 60-meter increase continuously throughout the first 7.5 meters of the trial, the velocity profile for the 7.5-meter dash starts to level off at around five meters.

<Figure 2>

On the basis of the fitted confidence intervals, velocity profiles of different target distances can be directly compared. *Figure 2B* shows the difference curve for the velocity profiles of the 7.5-meter dash and the 15-meter dash. The red (dotted) lines represent the range of positions for which the difference between the two velocity profiles (7.5-meter dash minus the 15-meter dash) is significantly different from zero. Beyond 5.2 meters, the average running velocity for the 7.5-meter dash is significantly lower than for the 15-meter dash. The average difference increases up to about -0.8 ms^{-1} towards the end of the trial. Based on the fitted values in *Figure 2A*, two other comparisons were made: The 7.5-meter dash versus the 30-meter dash and the 7.5-meter dash versus the 60-meter dash. Significant differences, comparable to those in *Figure 2B*, were found for both. Their respective observed windows of significant difference were: 5.2-7.5 meters and 5.0-7.5 meters. Following the same rationale, pair-wise comparisons were also made for the 15-meter dash and the 30-meter dash (*Table 1*, see also *Appendix A*). The results were consistent: Whenever participants closed in on the finish line, their running speeds declined. Here, we refrain from providing a full discussion on model specification, model performance and technical implementation of the various GAM-models. For now, note that all effects, fixed or random, were significant and that all models captured at least 99.4% of the variance.

Having established that a nonlinear pattern exists for sprint running in the context of interception *and* that target distance is only of influence on participants' velocity profiles in the context of sprinting towards a finish line, we will now attempt to characterize this non-linear relation, using participants' (maximum) running speed and acceleration as key variables.

<Table 1>

A new macroscopic model on the kinematics of sprint running

Figure 1 presents normalized running acceleration as a function of normalized running speed for each of the four target distances. Over the next paragraphs, we will take a closer look at participants' velocity-acceleration profiles to characterize the nonlinear patterns observed. A convenient and intuitive way to characterize the patterns observed in *Figure 1* would be with the use of polynomials. *Equation 1* provides a formulation for a family of functions that can be used to approximate acceleration ($\ddot{x}$, on the y-axis of *Figure 1*) as a function of running velocity ($\dot{x}$, on the x-axis of *Figure 1*) in maximal-effort sprint running (see also *Figure 3*).

$$\ddot{x} = a(\dot{x} + c)^{n-2} \cdot (\dot{x} - \dot{x}_{max})^2 \rightarrow \{\dot{x} \mid 0 \leq \dot{x} \leq \dot{x}_{max}\};\ a > 0;\ c > 0;\ n > 2 \quad (1)$$

Where a and c are constants, n is the total degree of the polynomial and $\dot{x}_{max}$ is the maximum running speed that an athlete can achieve. Changes in constant c cause horizontal stretching relative to point $\dot{x} = \dot{x}_{max}$, causing the polynomial to intersect the y-axis at greater values for $\ddot{x}$. When constant c equals zero the origin of the function lies at $(0,0)$. Changes in n cause the shape of the polynomial function to change (see also: *Figure 3*). Finally, the a-parameter is used to constrain the polynomial so that acceleration ($\ddot{x}$) is never greater than an athlete's maximal acceleration ($\ddot{x}_{max}$). Please note that a is not a 'free parameter' since it is constrained by the values of $\dot{x}_{max}$, $\ddot{x}_{max}$, n and c (see *Appendix B* for the derivation):

$$a = \frac{\ddot{x}_{max}}{\left(\frac{(n-2)\,\dot{x}_{max} - 2c}{n} + c\right)^{n-2}\left(\frac{(n-2)\,\dot{x}_{max} - 2c}{n} - \dot{x}_{max}\right)^{2}} \quad (2)$$

<Figure 3>

We performed an optimization procedure to find the optimal values for n and c. Optimization was performed on the basis of goodness of fit, assessed by the coefficient of determination (R^2). For optimization, processed data rather than raw data were used. The degree of the polynomial (n) was systematically varied between 2 and 10 with a step size of 0.1 and the horizontal stretch factor (c) was systematically varied between 0 and 100% of maximal running speed with a step size of 1%. The optimization procedure was executed separately for trials of the forward-condition and trials of the backward-condition. For every trial of every participant the coefficient of determination (R^2) was calculated. R^2's were then averaged over all trials of all participants to obtain an average coefficient of determination for every combination of n and c. With this procedure the best combination for n and c in terms of R^2 could be identified.

We found that a number of different combinations of n and c performed equally well (for both conditions). This was caused by an interdependence between n and c. An increase in n caused the apex of the polynomial to shift rightward, whereas an increase in c caused the apex of the polynomial to shift leftward. Thus, the effects of n and c cancel each other out when it comes to characterizing the local maximum in the data (see *Appendix C* for a visual illustration of this effect). Thus, solely based on the coefficient of determination, no principled decision could be made in selecting one combination of n and c over another. Given the present data set, there was one particular combination for n and c (for both conditions) that stood out when taking model complexity into account: $n = 3.2$, $c = 0$. For this combination, the effect for one of the two "free" parameters (c) is cancelled, thus effectively reducing the number of free parameters by half without loss of explanatory power. Based on this observation, we selected $n = 3.2$ and $c = 0$ to model the dynamics of sprint running, which simplifies *Equation 1* to hold[4]:

$$\ddot{x} = a\dot{x}^{1.2} \cdot (\dot{x} - \dot{x}_{max})^2 \rightarrow \{\dot{x} \mid 0 \leq \dot{x} \leq \dot{x}_{max}\};\ a > 0 \quad (3)$$

[4] Please note that the optimization procedure was performed only on data for which running velocity was greater than 1ms^{-1}. With the LPM-system, we could not accurately assess running speeds and accelerations below that threshold (see also the discussion section). So, for the present data, *Equation 3* is the most parsimonious. Future research, however, should point out whether *Equation 3* also holds for lower running speeds.

Using *Equation 3* to model acceleration in sprint running, the average coefficient of determination for trials of the forward-condition and for trials of the backward-condition was found to be 0.92 and 0.91, respectively.

<Table 2>

Next, we set out to validate *Equation 3* ($n = 3.2$). Through numerical simulation (Simulink, MathWorks) position, velocity, and acceleration were calculated from *Equation 3*. Preliminary inspection of the fits between the model and the data showed to be promising. *Figure 4* shows a representative trial for one participant performing a 30-meter dash in the forward-condition. The model closely approximates position (*Figure 4A*), velocity (*Figure 4B*) and acceleration (*Figure 4C*) over time. This close fit between the model and the data was further confirmed by calculating the coefficient of determination for all trials of the forward and backward conditions. Table 2 lists the average R^2-scores for position, velocity and acceleration, split out by target distance, for the forward-condition and the backward-condition. It is clear that the model provides a good description of the various kinematic measures that are related to performing a maximal-effort sprint. R^2-scores are even close to perfect for the distance-over-time relationship. When considering the average error in distance over time, for trials of the forward and the backward condition, the model was never off by more than 5.0% of the target distance both for the forward condition as well as for the backward condition. For the 60-meter dash of the forward condition, the model was even accurate within 1%, meaning that the model was never off by more than 37cm.

<Figure 4>

Forwards and backwards running compared

The data show that forward running and backward running are distinctly different in terms of absolute performance. Participants' peak running velocity was significantly higher [$t_{(30)}$ = 39.9, $p < 0.001$] in the forward running condition (M=7.63; SD=0.57) than in the backward running condition (M=5.20; SD=0.58). Similarly, participants' peak running acceleration was significantly higher [$t_{(30)}$ = 14.1, $p < 0.001$] in the forward running condition (M=4.58; SD=0.55) than in the backward running condition (M=3.35; SD=0.28). However, when looking at the way in which the macro-dynamics of running evolve over the course of a sprint, the apparent differences between forward running and backward running are disappear. Table 2 shows the goodness of fit for position, velocity, and acceleration for both forward running and backward running – hardly any differences in the coefficients of determination can be observed between both conditions. Thus, indicating that the macro-dynamics of forward running are highly similar in form to the macro-dynamics of backward running. The only difference between the two conditions is in the maximal velocities and accelerations that are obtained.

Individual differences in the kinematics of sprint running

Having validated the model, we now turn to its interpretation. How do maximal running speed and maximal running acceleration relate to influence the maximal distance that can be covered over time? Figure 5 shows the modelled action boundaries of all participants, with the slowest participant, the fastest participant and an average participant highlighted. From panel A, it can be seen that the fastest participant and the slowest participant are almost three seconds apart in crossing the 60-meter finish line. Looking at panel B, it can be seen that over the first two seconds, the faster participant develops speed faster than the slower participant. This development plateaus after about two seconds, as can also be seen from the acceleration

profiles in panel C. After about two seconds, the acceleration profiles of the fast and the slow participant start to converge and after three seconds the difference in acceleration between the fast and the slow participant is almost imperceptible. This means that around three seconds, participants have almost reached their top speed. Consequently, after that, all differences in performance are almost exclusively attributable to differences in top-speed. Before that, acceleration also plays a marked role (see also Figure 6).

<Figure 5>

This brings us to the final question of how maximal running speed and maximal running acceleration are related. Figure 6A shows a scatterplot of maximal running speed and maximal running acceleration ($R^2 = 0.58$). From the plot it can be seen that there is a moderate positive relationship between maximal running speed and maximal running acceleration: Participants that boast high peak-velocities typically also boast high peak-accelerations. The relationship however is not perfect. Participants can exhibit similar peak-velocities while exhibiting dissimilar peak-accelerations and vice versa. This phenomenon is highlighted in Figure 6A by the orange and cyan dyads, respectively. Using *Equation 3*, it can be demonstrated how individual differences in peak running velocity and peak running acceleration cause for markedly different running dynamics. From panels B, D, F and H, it can be seen how differences in *peak running velocity* translate to the macro-dynamics of running. The participant (in the orange dyad) with the greater top-speed covers more distance over time (panel B); has a higher overall running speed (panel D) and accelerates over a longer period of time (panel F). Finally, it can be seen that peak-acceleration is reached at a higher velocity for the faster runner than for the slower one. Close examination of panel B learns that after 1 second, the difference between the two runners is 0.05 meters; after 2 seconds this has increased to 0.47 meters and after 3 seconds this difference is 1.60 meters. Conversely, from panels C, E, G, and I of Figure 6, it can be seen how differences in *peak running acceleration* (cyan dyad) translate to the macro-dynamics of running. The runner with the greater acceleration covers more distance over time (panel C); has a higher overall velocity (panel E) and accelerates more intensely (panel G). While the difference in finish-time is less pronounced for the cyan pair than for the orange pair, the differences in the initial phases of the sprint are in fact more pronounced for the cyan pair. Whereas the orange pair differed 0.05 meter at 1 second and 0.47 meters at 2 seconds, the cyan pair differed 0.54 and 1.18 meters at those very same moments. At three seconds, the differences between the dyads are comparable again at 1.60 meters and 1.50 meters, respectively. Clearly, for short distances, having great accelerative capabilities pays off; while for larger distances having a great top-speed is favorable.

<Figure 6>

Discussion

The main finding of the present contribution is that the action boundary in maximal effort sprint running is determined by the current running speed of the agent in combination with their maximal running speed *and* maximal running acceleration. This finding is in line with previous research which showed that neither kinematic quality on its own could reliably capture the action boundary in running (Fajen et al., 2011; Oudejans et al., 1996; Postma et al., 2018). Furthermore, we found that the way maximal running speed and maximal running acceleration relate to determine the action boundary in running is unique for every individual. It was found that the moderate positive relationship between maximal running speed and maximal running acceleration harbored wide individual variation: Participants with

comparable maximal running speeds might show distinctly differing maximal accelerations, and vice versa. As such, the resulting locomotor boundaries are unique to every individual as well. Finally, we found that participants did not employ different pacing strategies for covering different target distances. Taken together, the present findings highlight the fact that action boundaries are individual-specific qualities that are dynamic in nature.

Model characteristics

While the results showed that the model was well able to characterize the kinematics of maximal effort sprint running, we were unable to accurately model the very first part of the sprint. More specifically, running speeds between 0 and 1 ms^{-1} could not accurately be measured (see also: Ogris et al., 2012; Stevens et al., 2014). As a result, the exact value of n and c could only be narrowed down to a *range* of possible values. Future research has to point out what the speed-acceleration profile looks like for the very first part of the sprint, so the *exact* value of n and c can be determined. The relevance of this endeavor would go beyond mere parameter optimization. The decision to engage in interceptive behavior is informed by (optic) information that specifies whether or not it is (still) within the agents' action possibilities to get to the future interception location in time. As such, an accurate characterization of agents' locomotor abilities at (near) standstill is needed to understand why agents initiate running under certain circumstances, but not in others.

Another issue pertaining to the characterization of the model is about the ecological grounding of its parameters: To what extent can the parameters of the model be traced back to behaviorally relevant characteristics of the agent-environment system? The answer to this question is two-fold. First, *maximal running speed* and *maximal running acceleration* as well as *current running speed* can be directly related to the agent: $\dot{x}_{max}$, $\ddot{x}_{max}$ and $\dot{x}$, respectively. Second, parameter a functions to set the local maximum of the curve such that it corresponds to the maximum rate of acceleration of the participant. This parameter is constrained by $\dot{x}_{max}$, $\ddot{x}_{max}$ and n (see also *Appendix B*). Together, these variables model the macro-dynamics of sprint-running in an ecologically valid manner. Still, a discussion is to be held about the order of the polynomial, n. As already mentioned above, we were unable to definitively characterize the order of the polynomial function, based on the current data. That is to say, based on our current analyses, the order of the model is estimated to lie between 3.2 and 6.9. Which makes that the choice for $n = 3.2$ was not motivated by ecological considerations but rather by modelling considerations, i.e., parsimony. Knowing agents' maximal acceleration at standstill would help to further constrain the polynomial function, allowing for a more ecological grounding of the order of the polynomial.

Finally, the model was specified such that it allowed for an accurate characterization of participants' accelerative qualities. Their decelerative qualities were not considered in the present context. Consequently, the model is not able to account for any decelerations that might be inherent to interceptive behaviors. The model is for instance unable to capture the finish-line effect or the slight oscillations in acceleration that can be observed when participants run at or near their maximal speed (see Figure 4C). Still, some interceptive behaviors might require rapid turns and quick starting and stopping. Such behaviors are prevalent in team sports, such as basketball. If one seeks to understand such behaviors, the model needs to be extended to include an account on the maximal rate of deceleration and the maximal rate of turning. It is likely that these three are dynamically related to one another: The maximal rate of turning and the maximal rate of deceleration are for instance dependent on current running speed. Future investigations should point out how these qualities relate to understand the action boundaries in agile (interceptive) behaviors.

Task ecology and representativeness

The aim of the present contribution was to model the action boundaries involved in interceptive behavior. To that end, we investigated various forms of sprinting that could be considered representative for the kind of running behavior that might be observed in interception tasks like running to catch a baseball and running to intercept an advancing quarterback. We investigated different modes of locomotion (forward and backward running) and we investigated various target distances. Still, the ecology of the current experimental setup was not fully representative of the task ecology (cf. Brunswick, 1956) of interceptive tasks like *fly-ball catching* and *gap-crossing*, implying that the results should be interpreted with care . Most interceptive tasks involve some form of coincidence timing (i.e., the temporal-spatial coordination of movement relative to something or someone). In the current experimental setup, the temporal aspect was not represented. While participants were told to get to the finish line as fast as possible, there were no demands on 'timing': any and all running speeds would eventually lead participants to cross the finish line. Put differently, their crossing of the finish line was not dependent on their temporal-spatial coordination relative to it. Besides this timing-element, social and competitive elements might have affected the representativeness of our task. From informal observations, we learned that participants tended to compete with others (even though this was never instructed). Such complex social interactions are likely not present, or present in a different way, when running to catch a fly ball. Together, such factors might have caused participants to organize their movements differently from the interceptive tasks we aimed to model. The extent to which the identified relationship is subject to task ecology is an (outstanding) empirical question. In future research, we aim to address this matter by recording (and modelling) maximal effort sprints for different task ecologies and evaluating their differences.

Implications for Affordance-Based Control modelling

Action boundaries play an important role in modelling Affordance-Based Control strategies (Fajen, 2007, 2013). Action boundaries separate action possibilities from action *im*possibilities. As such, having modelled the action boundary for running might proof a valuable first step towards the formulation of Affordance-Based Control models for interceptive behaviors. The present findings show that it is important to acknowledge the fact that (locomotor) action boundaries are dynamic in nature. Previous modelling attempts have often approximated action boundaries as fixed, singular values. The current results come to show that such approximations might not do justice to the biomechanical factors that limit our action possibilities. Further, it is important to recognize that the present model should not be taken to represent the affordance for interception just yet. Perception is of affordances (Gibson, 1979). Typically, affordances are specified as the ratio between some ideal value and a corresponding maximum in the same metric. For braking a car to a safe stop for instance, the affordance for safe stopping is specified as the ratio between ideal deceleration (d_{ideal}) and maximal deceleration (d_{max}); where ideal deceleration is the rate of deceleration that would bring a car to a safe stop without having to make additional braking adjustments (Fajen, 2005a, 2005c, 2005b, 2007). When the ratio of ideal deceleration over maximal deceleration is smaller than 1; safe braking is afforded. Conversely, when the ratio of ideal deceleration and maximal deceleration is greater than 1; safe braking is no longer afforded[5]. Through perceptual (re)calibration, motorists learn to relate ideal deceleration to maximal deceleration, allowing them to get better attuned to their environments and what it means to them in terms of safe braking. Similar principles might hold for interception as well, allowing

[5] It is important to note that ideal deceleration can be directly perceived by the motorist (Fajen, 2005a).

potential affordance-based control strategies for interception to be defined as the ratio of x_{ideal} over x_{max}. Where x is a placeholder for *speed*, *acceleration*, or some other (compound) kinematic measure. Once x_{ideal} has been captured in terms of its perceptual variables, it can be related to its corresponding action boundary. In the next paragraph, we will exemplify how this might work for an actual interception task by considering the fly-ball paradigm.

The fly-ball paradigm concerns the case of an outfielder running to catch a fly ball. To arrive at an affordance-based control strategy for the fly-ball paradigm, a measure is needed that perceptually specifies what action is required from the outfielder to make a successful catch (x_{ideal}). In case of the fly-ball paradigm, this required measure can be obtained from the work of Rozendaal & Van Soest (2003), who posited the *'exact Optical Acceleration Cancellation'* (exact OAC) strategy. From this strategy, the rate of acceleration that is required from the outfielder to get to the right place in the right time to make a catch (a_{ideal}) can be obtained[6]. Through perceptual calibration, a_{ideal} can be scaled to an outfielder's maximal acceleration, which we established in the present contribution, see Equation 3. This maximal acceleration can be denoted as a_{max}. Thus, affordance-based control for running to catch fly balls might be formalized as the ratio of ideal acceleration over maximal acceleration. When the ratio of a_{ideal} over a_{max} is smaller than 1; catching is afforded. Conversely, when the ratio of a_{ideal} over a_{max} is greater than 1; catching is *not* afforded.

To date, the problem in formalizing an affordance-based control strategy for running to catch fly balls has been the inability to accurately characterize outfielders' action boundaries. Previous studies have been unable to unequivocally pinpoint the variable(s) that limit catching performance in running to catch fly balls (Fajen et al., 2011; Oudejans et al., 1996; Postma et al., 2018). Equation 3 advances the state of the art by reliably modelling the action boundaries in sprint running (a_{max}), both for forward running as for backward running. As detailed above, pairing a_{max} to a_{ideal} would provide a first formalization of an affordance based control strategy in running to catch fly balls. Here, we do not wish to make any claims about the control strategies that outfielders use in practice rather, we wish to illustrate the merits of having characterized the action boundary for sprint running in the context of affordance-based control and interceptive tasks. Future research has to show whether outfielders indeed control their locomotor behavior in a way is consistent with the use of the ratio of a_{ideal} over a_{max}.

Conclusion

In the present contribution, we studied the dynamics of maximal-effort sprint running in the context of running to catch fly balls. The aim was to map the relation among maximum velocity, maximum acceleration, and the distance coverable over time. First, we established that Hill's model on the dynamics of running in athletic sprinting was not directly transferable to most interceptive tasks; a marked difference was observed between the dynamics of athletic sprinting and the dynamics exhibited by participants in the present study. This led us to propose an alternative model, specifically designed to capture the dynamics of sprinting, both forwards and backwards, in the context of interceptive tasks. With this model, we were able to make highly reliable predictions of participants' position-, velocity- and acceleration over time. Furthermore, using Generalized Additive Mixed Modelling, we were able to establish that target distance was of no profound influence on the

[6] In its original formulation, the rate of acceleration is not given in optical terms, but all terms can be captured in optical variables.

dynamics of sprint running, rendering our alternative model valid for target distances up to 60 meters. Finally, we showed that action boundaries are agent-specific and not to mention dynamic. Every individual has unique kinematic profiles that can be traced back to individual differences in kinematic qualities (e.g., maximal running speed and maximal running acceleration). With the present contribution, we have tried to ease the scientific process of formalizing Affordance-Based Control strategies for interception tasks. Also, the present work might also serve as a route-to-discovery for the specification of higher-order action boundaries.

Acknowledgements

We would like to thank FC Groningen for enabling us to collect data using the LPM-system. In this, special thanks go out to Wouter Frencken. Furthermore we would like to acknowledge Kyrill Visser, Niek de Boer and Pim Bos who worked diligently to help us collect the data. Finally, we thank the anonymous reviewers for their insightful comments.

Declaration of interest

The authors declare that they have no known competing financial interests or personal relationships that could have appeared to influence the work reported in this paper.

References

Brunswick, E. (1956). *Perception and the Representative Design of Psychological Experiments.* University of California Press. https://doi.org/10.1525/9780520350519

Fajen, B. R. (2005a). Calibration, information, and control strategies for braking to avoid a collision. *Journal of Experimental Psychology: Human Perception and Performance*, *31*(3), 480–501. https://doi.org/10.1037/0096-1523.31.3.480

Fajen, B. R. (2005b). Perceiving possibilities for action: On the necessity of calibration and perceptual learning for the visual guidance of action. *Perception*, *34*(6), 717–740. https://doi.org/10.1068/p5405

Fajen, B. R. (2005c). The scaling of information to action in visually guided braking. *Journal of Experimental Psychology: Human Perception and Performance*, *31*(5), 1107–1123. https://doi.org/10.1167/4.8.811

Fajen, B. R. (2007). Affordance-based control of visually guided action. *Ecological Psychology*, *19*(4), 383–410. https://doi.org/10.1080/10407410701557877

Fajen, B. R. (2013). Guiding locomotion in complex, dynamic environments. *Frontiers in Behavioral Neuroscience*, *7*, 85.

Fajen, B. R., Diaz, G., & Cramer, C. (2011). Reconsidering the role of movement in perceiving action-scaled affordances. *Human Movement Science*, *30*(3), 504–533. https://doi.org/10.1016/j.humov.2010.07.016

Furusawa, K., Hill, A. V., & Parkinson, J. L. (1927). Dynamics of "sprint" running. *Proceedings of the Royal Society of London B: Biological Sciences*, *102*(713), 29–42. https://doi.org/DOI: 10.1098/rspb.1927.0035

Gibson, J. J. (1979). *The ecological approach to visual perception.* (Eds.). Houghton, Mifflin and Company.

Hastie, T. J., & Tribshirani, R. J. (1990). *Generalized Additive Models* (1st ed.). Chapman and Hall.

Hill, A. V. (1927). *Muscular movement in man: The factors governing speed and recovery from fatigue.* McGraw-Hill Book Company, Inc.

Ogris, G., Leser, R., Horsak, B., Kornfeind, P., Heller, M., & Baca, A. (2012). Accuracy of the LPM tracking system considering dynamic position changes. *Journal of Sports Sciences*, *30*(14), 37–41. https://doi.org/10.1080/02640414.2012.712712

Oudejans, R. R. D., Michaels, C. F., Bakker, F. C., & Dolné, M. A. (1996). The relevance of action in perceiving affordances: Perception of catchableness of fly balls. *Journal of Experimental Psychology: Human Perception and Performance*, *22*(4), 879–891. https://doi.org/10.1037/0096-1523.22.4.879

Postma, D. B. W., Lemmink, K. A. P. M., & Zaal, F. T. J. M. (2018). The affordance of catchability in running to intercept fly balls. *Journal of Experimental Psychology: Human Perception and Performance*, *44*(9), 1336–1347. https://doi.org/10.1037/xhp0000531

Rozendaal, L. A., & Van Soest, A. J. K. (2003). Optical acceleration cancellation: A viable interception strategy? *Biological Cybernetics*, *89*(6), 415–425. https://doi.org/10.1007/s00422-002-0393-3

Steinmetz, S. T., Layton, O. W., Powell, N. V., & Fajen, B. R. (2020). Affordance-based versus current-future accounts of choosing whether to pursue or abandon the chase of a moving target. *Journal of Vision*, *20*(3), 1–19. https://doi.org/https://doi.org/10.1167/jov.20.3.8

Stevens, T. G. A., Ruiter, C. J. De, Niel, C. Van, Rhee, R. Van De, Beek, P. J., & Savelsbergh, G. J. P. (2014). Measuring acceleration and deceleration in soccer-specific movements using a Local Position Measurement (LPM) system. *International Journal of Sports Physiology and Performance*, *9*(3), 446–456.

https://doi.org/10.1123/IJSPP.2013-0340
Tagliamonte, S. A., & Baayen, R. H. (2012). Models, forests, and trees of York English: Was/were variation as a case study for statistical practice. In *Language Variation and Change* (Vol. 24, Issue 2). https://doi.org/10.1017/S0954394512000129
van Rij, J., Wieling, M., Baayen, R. H., & van Rijn, H. (2017). *Interpreting time series and autocorrelated data using GAMMs.* (R package version 2.3).
Wieling, M. (2018). Analyzing dynamic phonetic data using generalized additive mixed modeling: A tutorial focusing on articulatory differences between L1 and L2 speakers of English. *Journal of Phonetics*, *70*, 86–116. https://doi.org/10.1016/j.wocn.2018.03.002
Winter, B. (2013). Linear models and linear mixed effects models in R with linguistic applications. *CoRR*, *abs/1308.5*, 1–22. http://arxiv.org/abs/1308.5499
Winter, B., & Wieling, M. (2016). How to analyze linguistic change using mixed models, Growth Curve Analysis and Generalized Additive Modeling. *Journal of Language Evolution*, *1*(1), 7–18. https://doi.org/10.1093/jole/lzv003
Wood, S. N. (2003). Thin plate regression splines. *Journal of the Royal Statistical Society. Series B (Statistical Methodology)*, *65*(1), 95–114. https://doi.org/10.1111/1467-9868.00374
Wood, S. N. (2004). Stable and efficient multiple smoothing parameter estimation for generalized additive models. *Journal of the American Statistical Association*, *99*(99), 673–686. https://doi.org/10.1198/016214504000000980
Wood, S. N. (2011). Fast stable restricted maximum likelihood and marginal likelihood estimation of semiparametric generalized linear models. *Journal of the Royal Statistical Society. Series B (Statistical Methodology)*, *73*(1), 3–36. https://doi.org/10.1111/j.1467-9868.2010.00749.x
Wood, S. N. (2017). Generalized Additive Models. In *Statistical Computing: An Introduction to Data Analysis using S-Plus* (2nd ed.). Chapman and Hall/CRC.
Wood, S. N., Pya, N., & Säfken, B. (2016). Smoothing parameter and model selection for general smooth models. *Journal of the American Statistical Association*, *111*(516), 1548–1563. https://doi.org/10.1080/01621459.2016.1180986

Appendix A

Participants' running velocity declined towards the finish-line with an order of magnitude similar to the decline observed in *Figure 2*. With respect to differences in running velocity over the first 15 meters of the 15-, 30- and 60-meter dash, we found a significant window of difference (11.9 – 15 meters) for the comparison of the 15-meter dash with the 30-meter dash as well as a significant window of difference (11.6 – 15 meters) for the comparison of the 15-meter dash with the 60-meter dash. Leaving the comparison of running velocity over the first 30 meters of the 30-meter dash with the 60-meter dash. For this comparison, we found a significant window of difference of 25.9 to 30 meters. For all analyses presented here, the alpha-level was corrected for using a Bonferroni-correction.

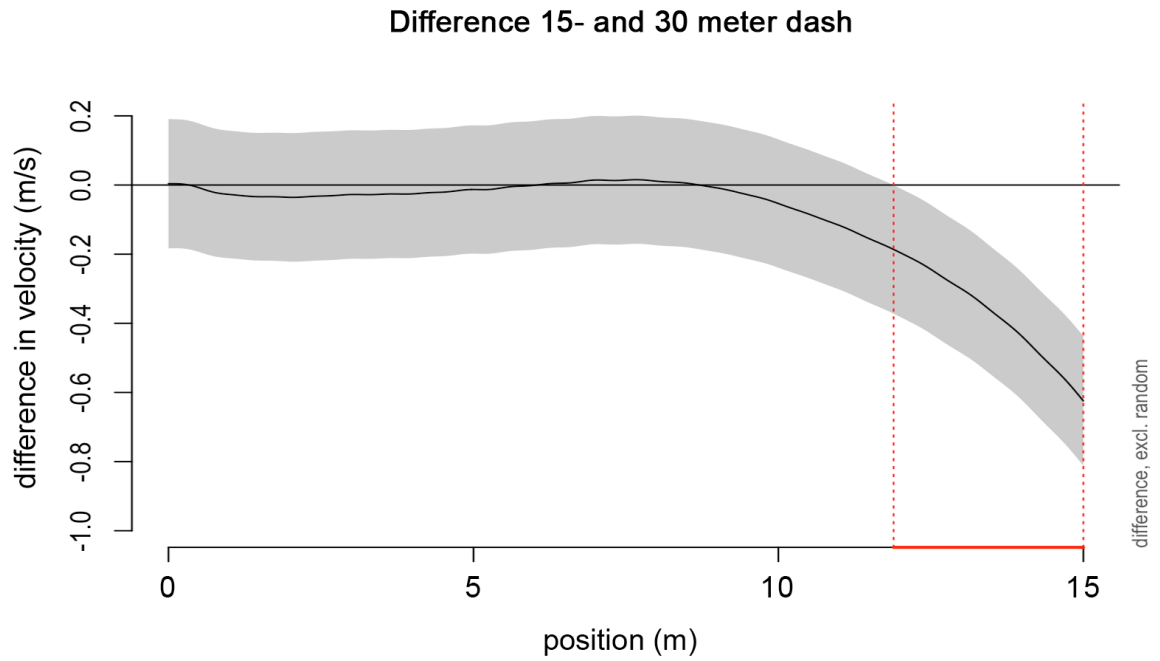

Figure A.1 | Difference curve for the velocity profiles of the 15-meter dash and the 30-meter dash. The average (curved line) and the 95% confidence interval (shaded region) are provided. Position (m) is on the abscissa and the estimated difference in velocity (m/s) is on the ordinate. The area demarcated by the red (dotted) lines represents the range of positions for which the difference between the velocity profiles (15-meter dash minus 30-meter dash) is significantly different from zero.

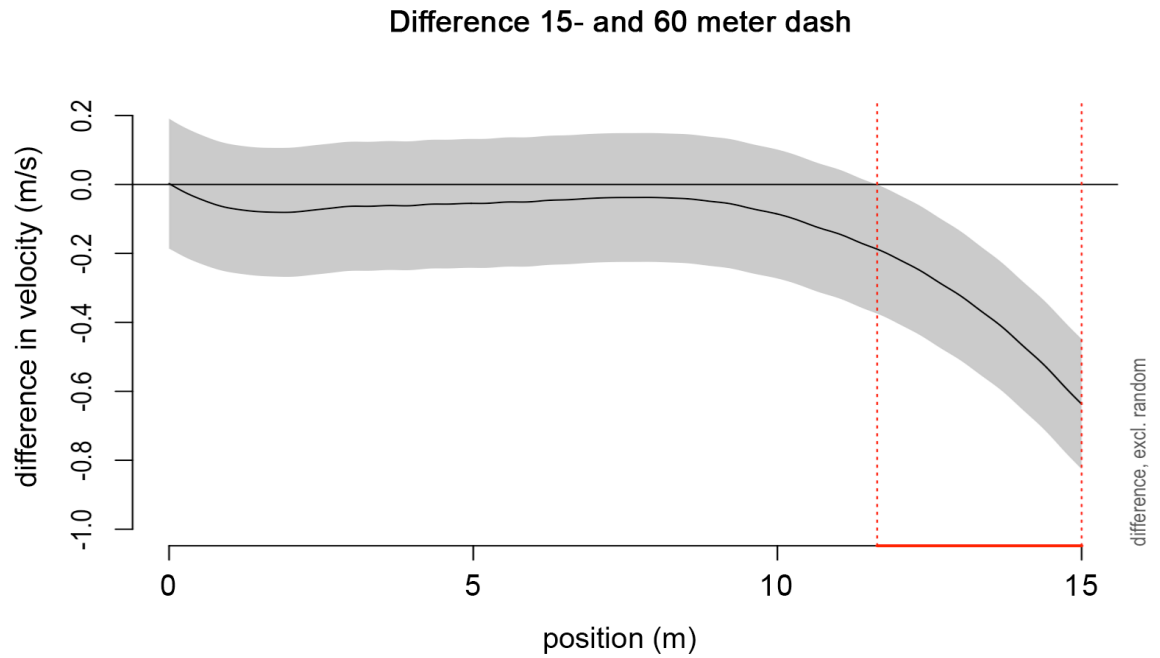

719
720 **Figure A.2 | Difference curve for the velocity profiles of the 15-meter dash and the 60-meter dash. The average (curved**
721 **line) and the 95% confidence interval (shaded region) are provided. Position (m) is on the abscissa and the estimated**
722 **difference in velocity (m/s) is on the ordinate. The area demarcated by the red (dotted) lines represents the range of**
723 **positions for which the difference between the velocity profiles (15-meter dash minus 60-meter dash) is significantly**
724 **different from zero.**

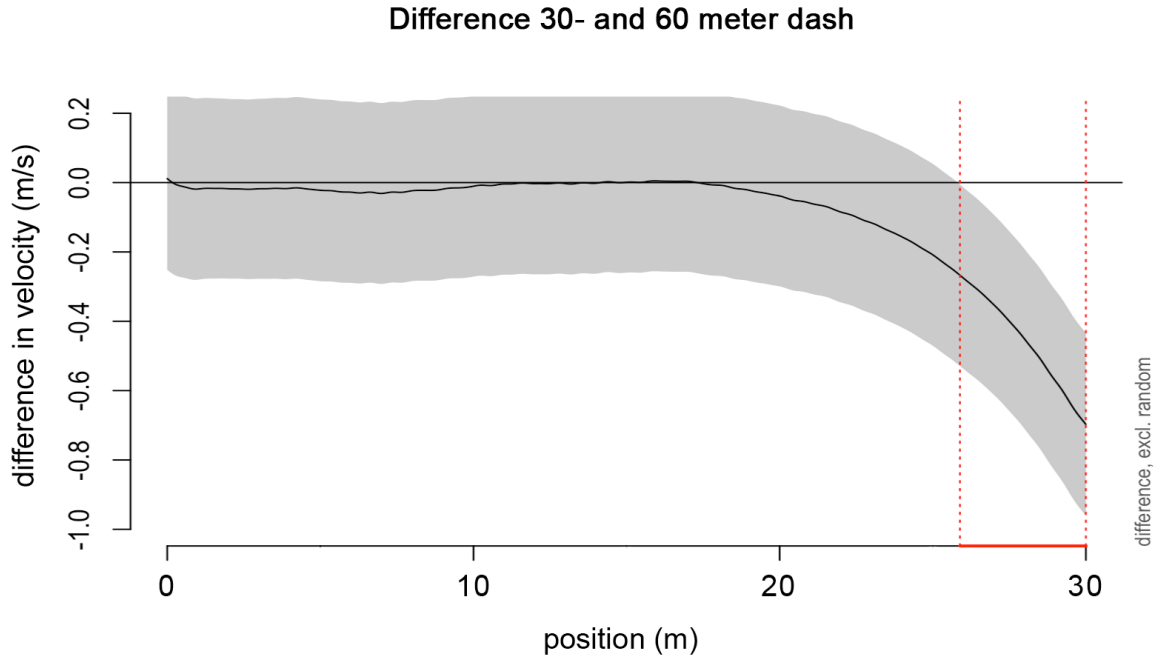

725
726 **Figure A.3 | Difference curve for the velocity profiles of the 30-meter dash and the 60-meter dash. The average (curved**
727 **line) and the 95% confidence interval (shaded region) are provided. Position (m) is on the abscissa and the estimated**
728 **difference in velocity (m/s) is on the ordinate. The area demarcated by the red (dotted) lines represents the range of**
729 **positions for which the difference between the velocity profiles (30-meter dash minus 60-meter dash) is significantly**
730 **different from zero.**

731

Appendix B

The a-parameter can be derived by setting the first derivative of *Equation 4* to zero and solving for $\dot{x}$, providing:

$$\dot{x} = \frac{(n-2)\,\dot{x}_{max} - 2c}{n} \tag{A.1}$$

Equation A1 provides the $\dot{x}$-coordinate for which $\ddot{x} = \ddot{x}_{max}$. Knowing the $\dot{x}$-coordinate for which $\ddot{x}$ is maximal allows for the a-parameter in *Equation 4* to be established. For $\ddot{x} = \ddot{x}_{max}$, the a-parameter is given by:

$$a = \frac{\ddot{x}_{max}}{\left(\frac{(n-2)\,\dot{x}_{max} - 2c}{n} + c\right)^{n-2}\left(\frac{(n-2)\,\dot{x}_{max} - 2c}{n} - \dot{x}_{max}\right)^{2}} \tag{A.2}$$

Subsequently entering *Equation A2* into *Equation 4* provides:

$$\ddot{x} = \frac{\ddot{x}_{max}}{\left(\frac{(n-2)\,\dot{x}_{max} - 2c}{n} + c\right)^{n-2}\left(\frac{(n-2)\,\dot{x}_{max} - 2c}{n} - \dot{x}_{max}\right)^{2}}(\dot{x} + c)^{n-2}(\dot{x} - \dot{x}_{max})^{2} \tag{A.3}$$

Equation A3 is a reformulation of *Equation 4* in which the a-parameter is described in terms of: $\ddot{x}_{max}$, $\dot{x}_{max}$, n and c.

Appendix C

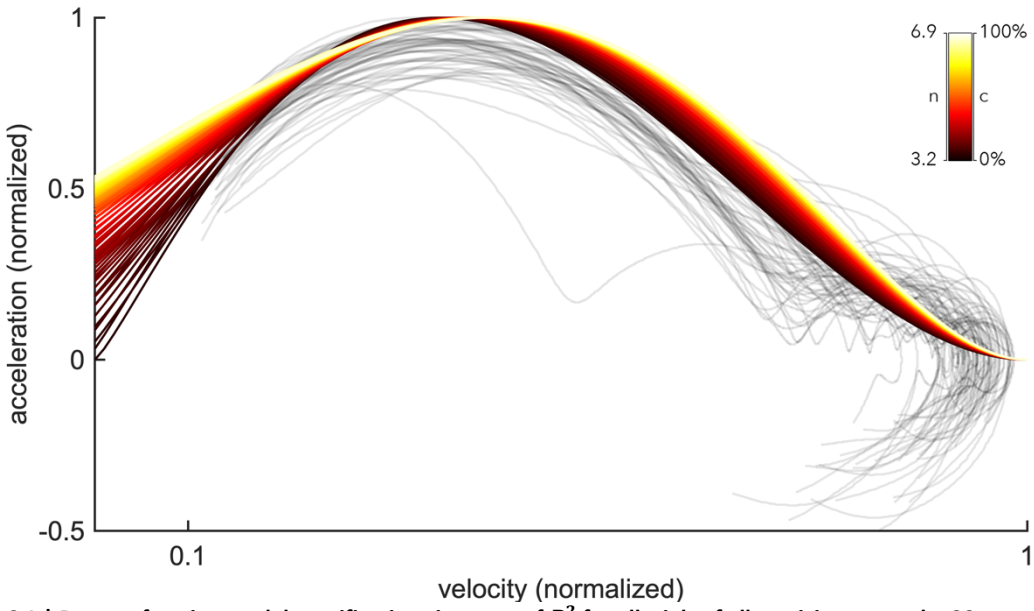

Figure C.1 | Best performing model specifications in terms of R^2 for all trials of all participants on the 30-meter dash of the forward-condition, with running velocity on the abscissa and running acceleration on the ordinate. Both running velocity and acceleration have been normalized by scaling all values to participants' maximal running velocity and acceleration, respectively. Semitransparent black lines represent participants' data, colored lines represent different model specifications (i.e. different values for n and c). A red-yellow gradient is used to represent different model specifications; the red side of the spectrum specifies low values for n and c (from: $n = 3.2$ and $c = 0$) and the yellow side of the spectrum specifies higher values for n and c (up to: $n = 6.9$ and $c = 100\%$).

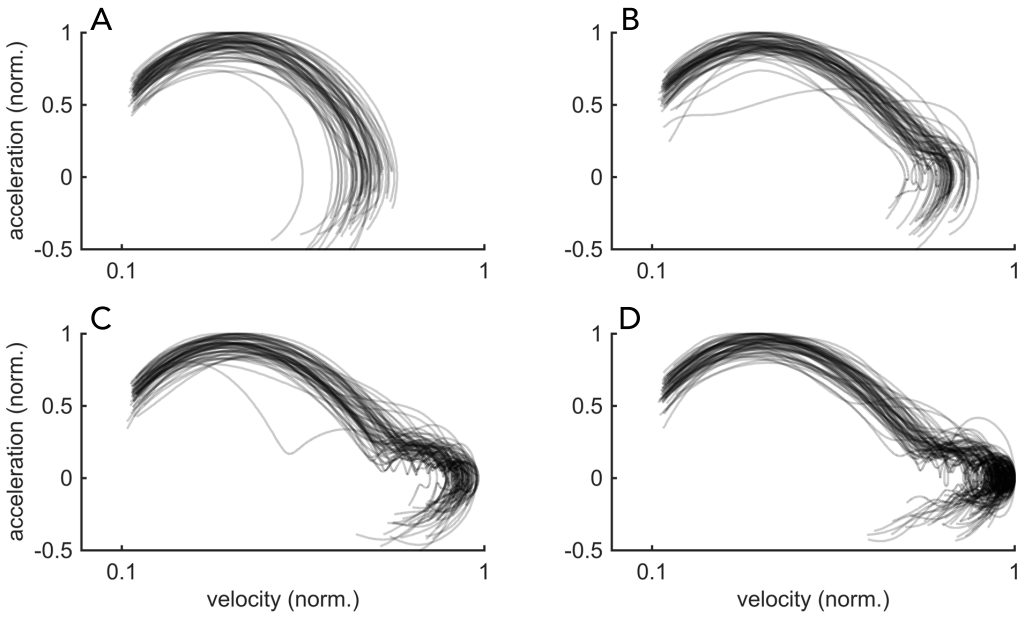

Figure 1 | Sprint profiles from the forward-condition (condition 1). Normalized running velocity is on the abscissa and normalized running acceleration is on the ordinate. Both running velocity and acceleration have been normalized by scaling all values to participants' maximal running velocity and acceleration, respectively. The velocity-acceleration profiles are split out by target distance: Panel A represents all trials from the 7.5-meter dash; panel B represents all trials from the 15-meter dash; panel C represents all trials from the 30-meter dash, and panel D represents all trials from the 60-meter dash.

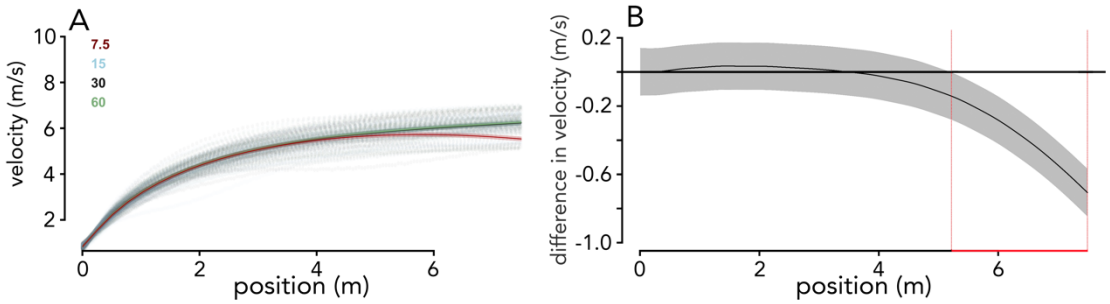

Figure 2 | A) Velocity profiles over the first 7.5 meter for sprints with different target distances: 7.5-meter dash (red), 15-meter dash (cyan), 30-meter dash (dark grey) and 60-meter dash (green). Dotted curves represent measured running speed for different target distances, while unbroken curves, with 95% confidence intervals, represent fitted values. Generalized Additive Modeling was used to determine the fitted values. B) Difference curve for the velocity profiles of the 7.5-meter dash and the 15-meter dash. The average (curved line) and the 95% confidence interval (shaded region) are provided. Position (m) is on the abscissa and the estimated difference in velocity (m/s) is on the ordinate. The area demarcated by the red (dotted) lines represents the range of positions for which the difference between the velocity profiles (7.5-meter dash minus 15-meter dash) is significantly different from zero.

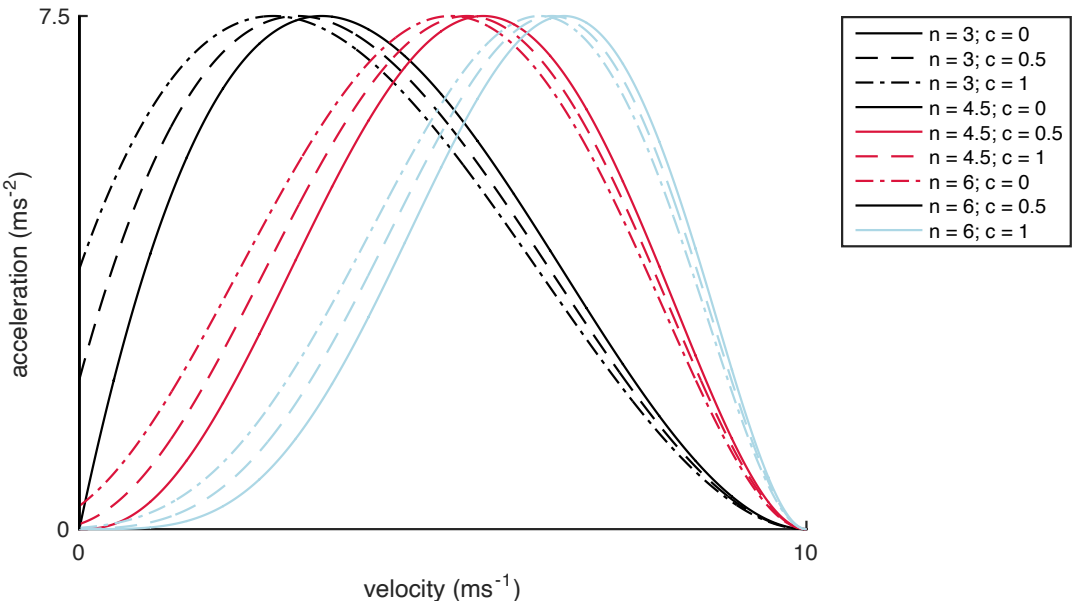

Figure 3 | Exemplary plot showing polynomials of the form specified by Equation 4. The polynomial functions displayed here differ in order (n) and in constant (c). In this example, the α-parameter was calculated, for every combination of n and c, to keep maximum running velocity ($\dot{x}_{max}$) and maximum running acceleration ($\ddot{x}_{max}$) constant at 10ms^{-1} and 7.5 ms^{-2} respectively.

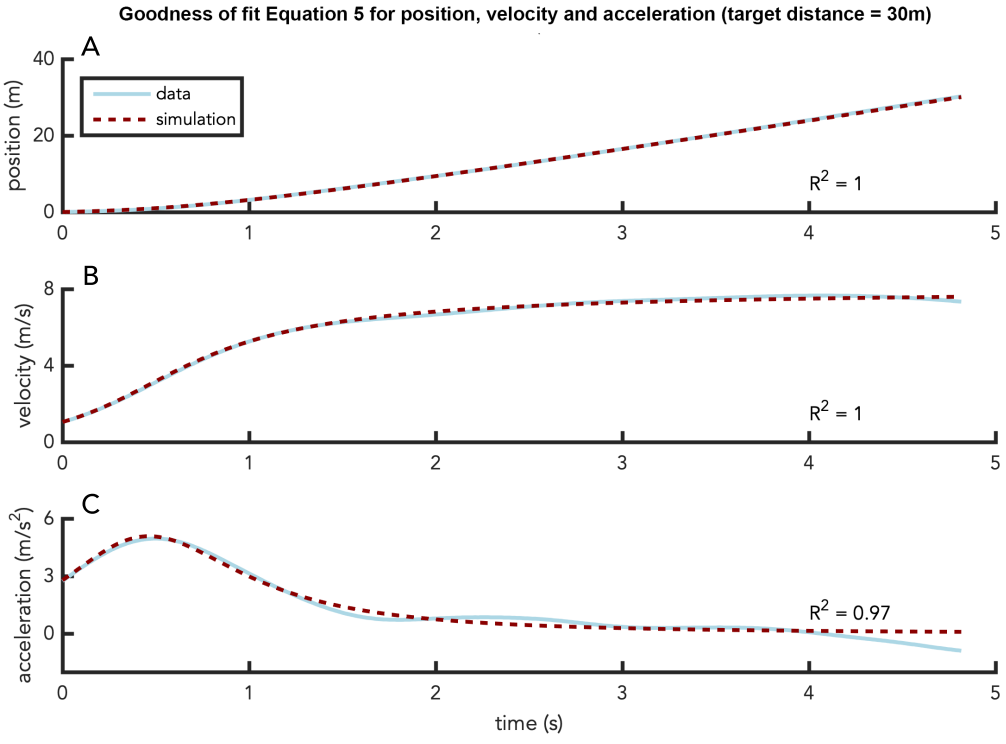

Figure 4 | Time series data of position (A), velocity (B) and acceleration (C) for one representative trial (forward-condition, 30-meter dash). The solid blue lines represent the data and the red dashed lines represent the model's simulation. Goodness of fit (R^2) is provided for each kinematic measure.

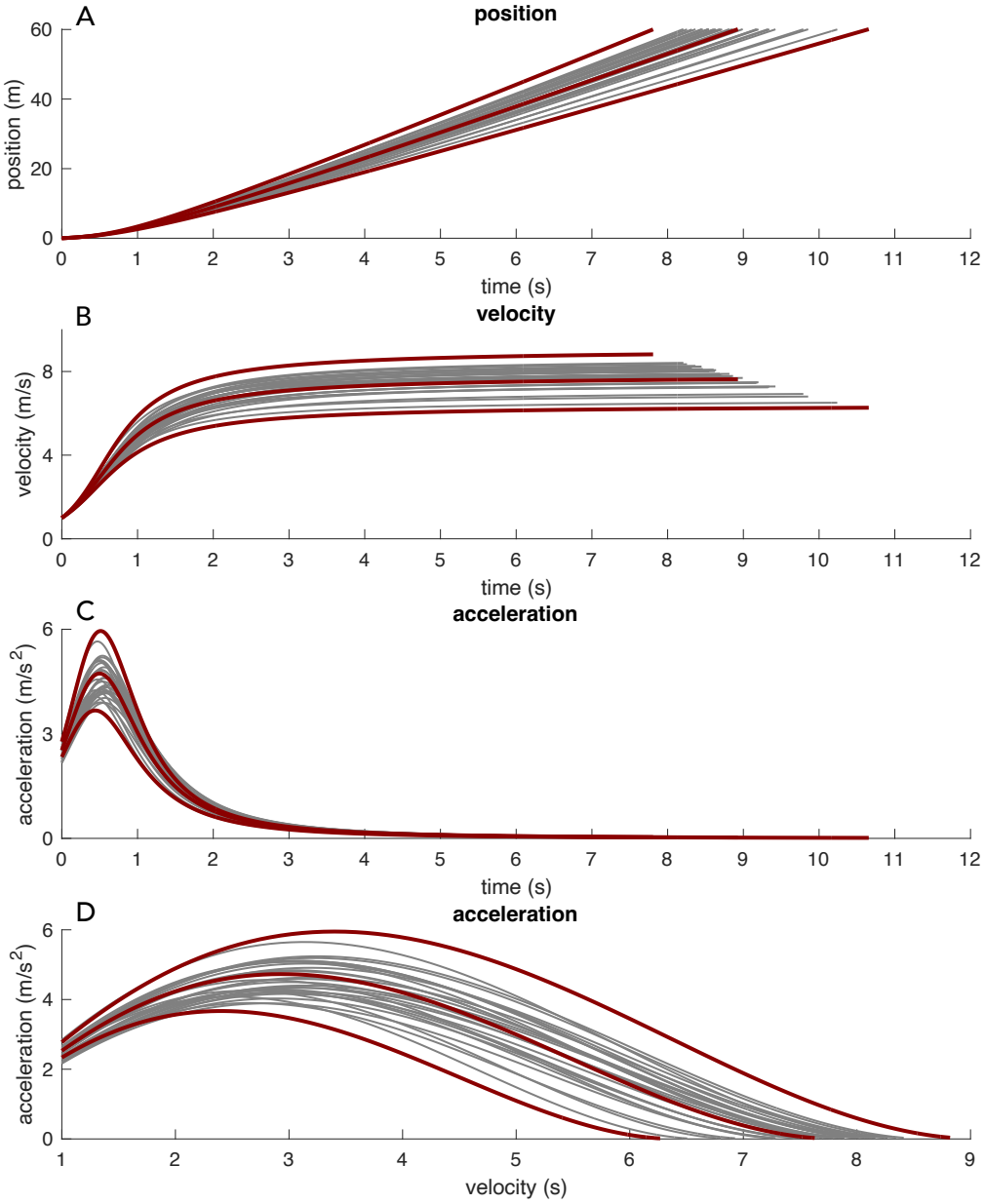

Figure 5 | Modelled action boundaries of all participants expressed in terms of position (panel A); velocity (panel B); acceleration (panel C) and acceleration-over-velocity (panel D). The bold lines in red highlight the fastest participant (upper line), the slowest participant (lower line) and an average participant (middle line).

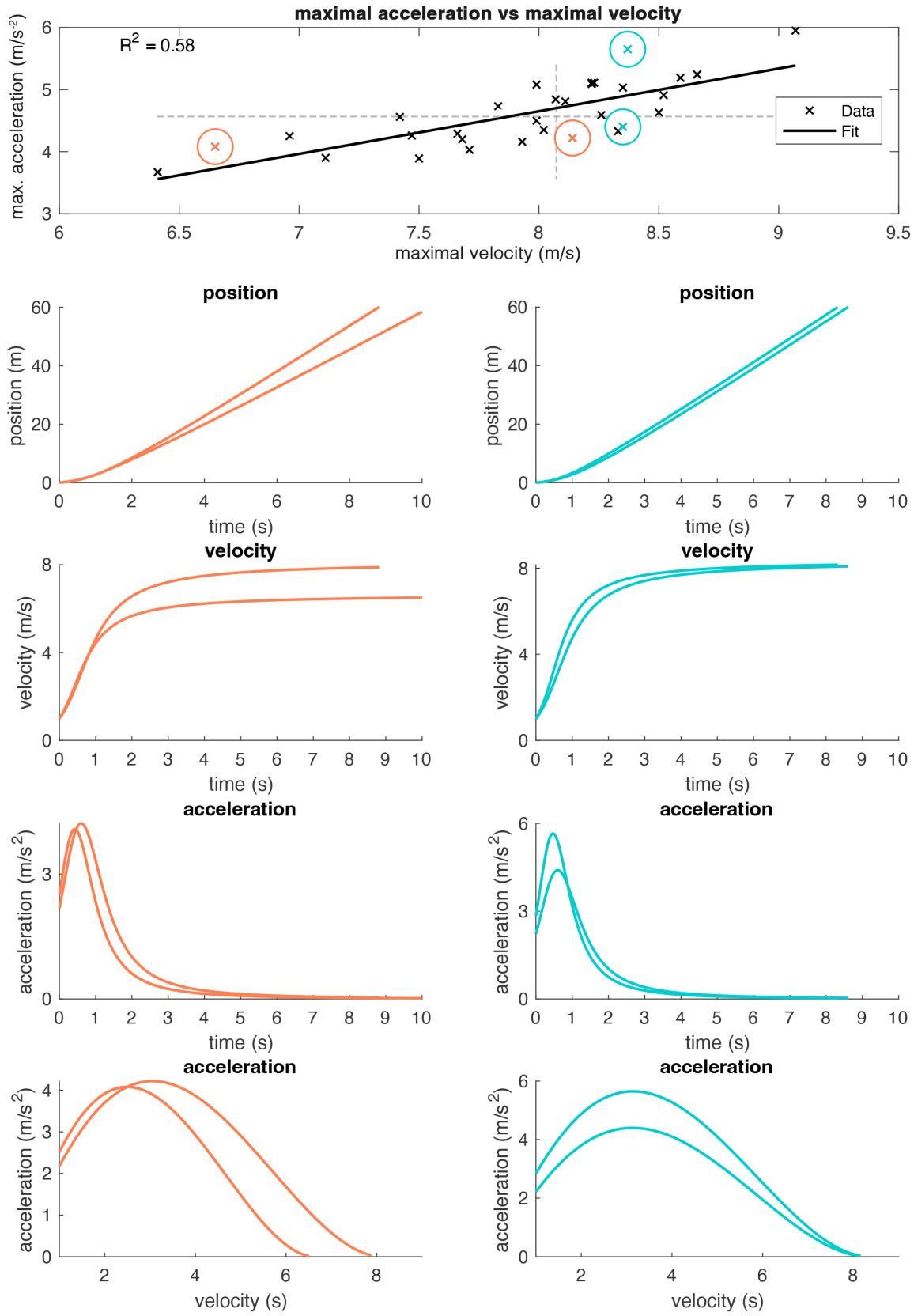

Figure 6 | Compound figure showing the relationship between maximal running velocity, maximal running acceleration and the distance coverable over time for forward running. Panel A shows a scatterplot of the *observed* maximal running velocity and acceleration of participants. Dashed lines represent the median values for running speed (vertical) and running acceleration (horizontal). Exemplary dyads are highlighted for illustrational purposes. The members of the orange dyad have similar values for peak-acceleration and dissimilar values for peak-velocity. The members of the cyan

dyad have similar values for peak-velocity and dissimilar values for peak-acceleration. Panels B-I show the *modeled* macro-dynamics of sprint-running for the orange dyad (left-hand side) and the cyan dyad (right-hand side). The action boundaries for both dyads are illustrated in terms of position (panel B and C); velocity (panel D and E); acceleration (panel F and G); and acceleration-over-velocity (panel H and I). The orange graphs represent the orange dyad, and the cyan graphs represent the cyan dyad.

Table 1 | Pair-wise comparison of velocity profiles

	Comparator Target Distance		
Target Distance	15m	30m	60m
7.5m	*2.3*	*2.3*	*2.5*
15m	-	*3.1*	*3.4*
30m	-	-	*4.1*

Note. This table shows the extent of the observed 'finish-line effect' for different target distances. That is, this table shows the distance to the finish line for which the velocity profiles of any two target distances were significantly different from zero (window of significant difference). For example, the velocity profiles of the first 7.5 meters of the 7.5-meter dash were significantly different from the velocity profiles of the first 7.5 meters of the 15-meter sprint for the final 2.3 meters to reaching the finish line (first row, first column).

Table 2 | Model goodness of fit (R^2) for position, velocity and acceleration for different target distances and running directions

	Target Distance							
	Forward				Backward			
	7.5m	15m	30m	60m	3.75m	7.5m	15m	30m
Position	1.00	1.00	1.00	1.00	1.00	1.00	1.00	1.00
Velocity	0.98	0.99	0.98	0.95	0.98	0.98	0.97	0.95
Acceleration	0.93	0.94	0.90	0.91	0.94	0.94	0.89	0.87